Olivares, J., Pastén, C., Monsalve, K., Novoa, G. and Gesche, R. (2025). Seismic coefficients adopted in the design of Chilean tailings dams. *Obras y Proyectos* **38**, 4-26, https://doi.org/10.21703/0718-2813.2025.38.3628

Seismic coefficients adopted in the design of Chilean tailings dams

Coeficientes sísmicos adoptados en el diseño de presas de relaves chilenas

Fecha de entrega: 23 de marzo 2025
Fecha de aceptación: 2 de julio 2025

Jaime Olivares[1], César Pastén[1], Karina Monsalve[2], Gullibert Novoa[2] and Roberto Gesche[1]

[1] University of Chile, Department of Civil Engineering, Av. Blanco Encalada 2002, Santiago, Chile, jaime.olivares@ug.uchile.cl, cpasten@uchile.cl (https://orcid.org/0000-0002-6683-0619), rgesche@uchile.cl

[2] Servicio Nacional de Geología y Minería de Chile, Department of Mine Safety, karina.monsalve@sernageomin.cl, gullibert.novoa@sernageomin.cl

The design of tailings dams considers a pseudo-static stability analysis using the limit equilibrium method, where inertial effects are captured by forces proportional to the weight of the sliding mass and seismic coefficients. This study compiles and analyzes a database of horizontal seismic coefficients (k_h) adopted in the design of 125 tailings dams built in Chile from 1983 to 2022. The database also considers geometric, seismic, and geotechnical information that influences the factors of safety obtained in slope stability analyses. This study reviews 11 methods adopted for the estimation of k_h and recommends a range of values for design earthquakes.

Keywords: seismic coefficients, tailings dams, pseudo-static analysis

El diseño de presas de relaves considera un análisis de estabilidad pseudoestático mediante el método de equilibrio límite, donde los efectos inerciales se capturan mediante fuerzas proporcionales al peso de la masa deslizante y a los coeficientes sísmicos. Este estudio recopila y analiza una base de datos de coeficientes sísmicos horizontales (k_h) adoptados en el diseño de 125 presas de relaves construidas en Chile entre 1983 y 2022. La base de datos también considera información geométrica, sísmica y geotécnica que influye en los factores de seguridad obtenidos en los análisis de estabilidad de taludes. Este estudio revisa 11 métodos adoptados para la estimación de k_h y recomienda un rango de valores para sismos de diseño.

Palabras clave: coeficientes sísmicos, presas de relaves, análisis pseudoestático

Introduction

Tailings storage facilities (TSFs) are designed to safely impound large volumes of mine waste. The optimal design and performance evaluation of these structures is a matter of concern since larger TSFs are being built, increasing the consequences in case of a breach (Bowker and Chambers, 2015), such as the recent high-profile failures in Canada (Mount Polley, 2014) and Brazil (Samarco 2015 and Brumadinho 2019) (Williams, 2021).

Chile has 791 TSFs according to the National Geology and Mining Service (Sernageomin, 2024), being the third in the World behind China with 5189 TSFs (Tang *et al*., 2020) and the United States with 1635 TSFs (US Army Corps of Engineers, 2019). Currently, the design, construction, and operation of the TSFs is ruled by the Supreme Decree Nº 248 (DS248, Ministerio de Minería, 2007) and the Decree Nº 50 (D50, Ministerio de Obras Públicas, 2015). These standards require several analyses to verify the physical stability of tailings dams, including slope stability analyses, numerical dynamic analyses, detailed geotechnical characterization, and seismic hazard studies.

The DS248 mandates physical stability analyses in four phases. Phase I consists of pseudo-static analyses using the limit equilibrium method, assuming total liquefaction of the impounded tailings. In Phase II, pseudo-static analyses consider a simplified estimate of pore water pressures. Phase III requires dynamic analyses with numerical

simulations to estimate seismic displacements. Finally, Phase IV considers analyses for the TSF closure condition, considering a design earthquake, that can be equivalent to a maximum credible earthquake (MCE), and aging effects on material properties. Regarding stability verifications in Phases I and II, the minimum required pseudo-static factor of safety is $FoS_{PS} = 1.2$ for the design earthquake.

The D50 classifies TSFs according to dam height and impounded tailings volume as shown in Table 1. The stability of TSFs, according to the D50 standard, is evaluated as follows. For class-A dams, static and pseudo-static analyses are required where simplified methods can be used to obtain the horizontal peak ground acceleration (PGA). For class-B dams, static and pseudo-static analyses are needed for the MCE and the design earthquake. The MCE is defined as the largest earthquake that can occur in a site, because of a recognized tectonic fault or because it is located within a certain seismotectonic region and framework. This earthquake can cause the largest ground shaking, for which the facility should be designed or evaluated. A dam should not experience a sudden collapse or uncontrolled release if subjected to the MCE although tolerable dam damage and adjoining facilities is accepted. The design earthquake is the one that causes a ground shaking resulting in minor and acceptable dam damage, appurtenant structures, and equipment, without interrupting the operation of the facility. The associated return period should not be lower than 475 years. The design earthquake is considered in this study as the operating basis earthquake (OBE). The need to include dynamic analyses in the stability evaluation of class-B dams depends on the seismicity of the area, the type of dam, its foundation soil, and other characteristics that must be duly justified in the project. For class-C dams, static stability analyses and dynamic analyses are required. These last analyses should be performed with ground motion records of Chilean earthquakes of magnitudes larger than $Ms = 8.5$. In this case, pseudo-static stability analyses are not required. Regarding the stability verification, the minimum required static factor of safety is $FoS_{ST} = 1.4$ and the minimum pseudo-static factor of safety is $FoS_{PS} = 1.2$. In addition, the post-seismic stability of class-B and -C dams should be verified and comply with a minimum factor of safety $FoS_{P} = 1.0$.

Table 1: Dam class according to the D50

Class	Dam maximum height, H	Impounded volume, Vol
A	$5\ m < H < 15\ m$	$50.000\ m^3 < Vol < 1.500.000\ m^3$
B	$15\ m \leq H < 30\ m$	$1.500.000\ m^3 \leq Vol < 60.000.000\ m^3$
C	$H \geq 30\ m$	$Vol \geq 60.000.000\ m^3$

In the pseudo-static analysis, the horizontal force that represents the inertial force during an earthquake is expressed as the product of a horizontal seismic coefficient (k_h) and the weight of a potential sliding mass. For the seismic coefficient to properly capture the seismic stability of a tailings dam, several critical factors must be considered, such as the characteristics of the earthquake ground motion, the seismic amplification of the dam, the geotechnical material properties (*e.g.*, the shear strength parameters and the mass density), as well as the location, the geometry, the static factor of safety, and the stiffness of the sliding mass (Duncan *et al*., 2014; Seed and Martin, 1966).

The most classical approaches to estimate seismic coefficients reviewed in the literature (*e.g.*, Duncan *et al*., 2014; Kramer, 1996) recommend seismic coefficients as a function of the earthquake magnitude, the peak ground acceleration (PGA), the pseudo-static factor of safety, the tolerable sliding mass displacement, and the extend of the material strength reduction during cyclic loading.

This study focuses on compiling and analyzing a database of k_h adopted in the design of 125 tailings dams in Chile from 1983 to 2022. The database considers geometrical features of the dams, as well as design considerations, such as operational and maximum credible earthquakes, peak ground accelerations, earthquake mechanisms (interface, inslab, and shallow crustal), static and pseudo-static factors of safety, and seismic displacements, when available. The study revises the different methods adopted in the evaluation of k_h and the seismic performance of a group of dams subjected to large subduction earthquakes in the last decades. The study aims at supporting the selection of k_h in future designs of tailings dams based on the experience of the past 40 years.

Methods for estimating seismic coefficients

This section describes the methods to estimate k_h considered

in the design of the 125 TSFs compiled in the database presented in Table A1 in the Annex.

Method 1 – Saragoni (1993)

Saragoni's (1993) method was developed in a seismic risk report for the reconstruction of the Port of Valparaíso after the 1985 M_w 8.0 Valparaíso Earthquake (Ruiz and Madariaga, 2018). This method modified Noda and Uwave's (1976) equation (1), which defined k_h as a function of the peak ground acceleration (PGA) and the acceleration of gravity (g).

$$k_h = \begin{cases} \frac{PGA}{g} & PGA \leq 0.2g \\ \frac{1}{3}\left(\frac{PGA}{g}\right)^{\frac{1}{3}} & PGA > 0.2g \end{cases} \quad (1)$$

This equation was developed based on the seismic failure of several gravity quay walls in Japanese port facilities, assuming the quay walls were in a limit equilibrium state (*i.e.*, $FoS_{PS} \sim 1.0$). The PGAs were inferred from ground motion models developed from ground shakings recorded with Japanese SMAC-type accelerographs that were unable to adequately record high frequency motions, hence, underpredicting the PGA. Saragoni (1993) proposed a method to correct PGA recorded from SMAC accelerographs to a PGA recorded from Kinemetrics SMA-1 accelerographs, which have improved high frequency resolution and were used in Chile at the time. The ratio between PGA estimated from SMA-1 and SMAC accelerographs was estimated at 3.31. Then, equation (1) was modified to determine k_h from PGA recorded from Kinemetrics SMA-1 accelerographs as

$$k_h = \begin{cases} 0.3\frac{PGA}{g} & PGA \leq 0.67g \\ 0.22\left(\frac{PGA}{g}\right)^{\frac{1}{3}} & PGA > 0.67g \end{cases} \quad (2)$$

This method is usually applied considering the PGA estimated from seismic hazard studies.

Method 2 – Decree No. 86 (1970)

The Decree Nº 86 (D86, Ministerio de Minería, 1970) regulated the construction and operation of tailings dams in Chile from 1970 to 2007, before the enactment of the DS248 in 2007. D86 defined the k_h in equation (3) as a function of the number of inhabitants (N) within a critical zone determined by the hazardous distance (D_h) after the tailings facility closure.

$$k_h = 0.05 \log(100 + N) \quad (3)$$

The hazardous distance (D_h) in equation (4) is calculated as a function of the tailings tonnage susceptible to liquefaction T (tons) and the slope of the natural terrain downstream the tailings facility i (%).

$$D_h = 2 \cdot 10^{-6} T \cdot i \text{ [km]} \quad (4)$$

This method was intended only for designs that considered the OBE. The minimum k_h obtained when no population is affected downstream of the tailings facility is $k_h(N = 0) = 0.1$.

Method 3 – Guidelines DS248 (2016)

Sernageomin published guidelines for the correct use of the technical aspects of the DS248 targeted to small mining projects producing less than 5.000 tons/month (Sernageomin, 2016). The guidelines recommended the estimation of k_h as a function of the maximum effective acceleration (A_0) defined in the Chilean building seismic design standard (NCh 433, Instituto Nacional de Normalización, 2012).

$$k_h = 0.5\frac{A_0}{g} \quad (5)$$

The A_0 depends on the seismic zone where the tailings facility is located. The NCh433 divides the Chilean territory into three seismic zones (Figure 1(a)) based on a regional seismic hazard assessment that considers the historic seismicity, as well as the geologic and seismological framework of the country. The coastal Zone 3 is assigned $A_0 = 0.4g$, the central valleys Zone 2 is assigned $A_0 = 0.3g$, and the mountains Zone 1 is assigned $A_0 = 0.2g$. Hence, the k_h considered in the guidelines for Zones 3, 2, and 1 are $k_h = 0.2$, 0.15, and 0.1, respectively. This method was intended for designing against the MCE, but the Chilean Highway

Manual (Ministerio de Obras Públicas, 2020) considered the same equation for the design of earth retaining structures subjected to OBE. It is worth noting that the A_0 is not the PGA.

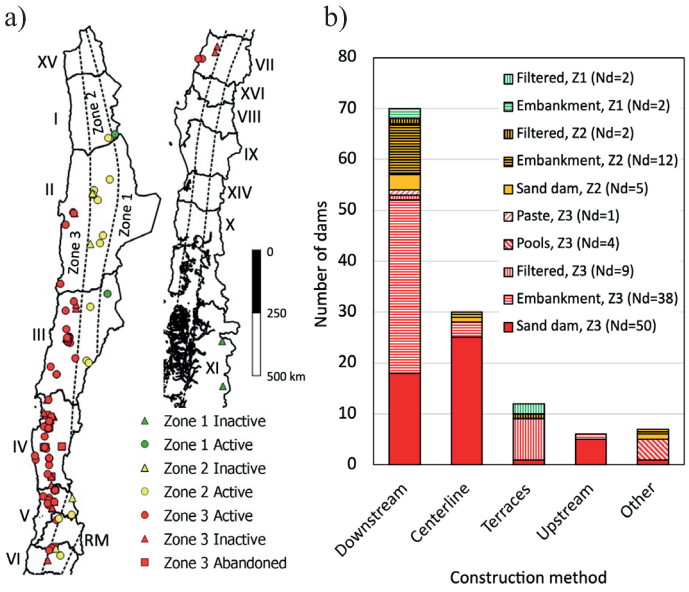

Figure 1: a) Spatial distribution of the 125 analyzed tailings dams in Chile, considering the three seismic zones (1, 2, and 3) of the NCh433 standard and the TSFs status (active, inactive, and abandoned). b) Construction methods and type of TSF (embankment, sand dam, filtered, paste, and pool). Nd: number of dams, Z1: zone 1, Z2: zone 2, and Z3: zone 3.

Method 4 – NCh433 (1996)

This method assumes that k_h is equal to the maximum seismic coefficient (C) of the NCh433 standard (Table 6.4 in the standard), which is used to calculate the basal shear stress in building design. C depends on the response modification factor R, which reflects the energy absorption and dissipation characteristics of a building, and the S coefficient that depends on the seismic site classification, ranging from rock and cemented soil sites (Type A) to soils of medium compaction or medium consistency (Type E). The S coefficient can adopt values S = 0.9, 1.0, 1.05, 1.2, and 1.3 for soil types A, B, C, D, and E, respectively (Ministerio de Vivienda y Urbanismo, 2011). Equation (6) shows the k_h estimated as the maximum seismic coefficient C for R = 2, according to the NCh433 standard.

$$k_h = C = 0.9S\frac{A_0}{g} \tag{6}$$

In some of the analyzed cases, 0.9S is set to unity, leading to k_h depending exclusively on A_0. The use of this method is associated to the design for the MCE.

Method 5 – Fraction of PGA

This method estimates k_h as a fraction α of the PGA (equation (7)), where α is a constant that ranges from 1/3 to 1.

$$k_h = \alpha\frac{PGA}{g} \tag{7}$$

The PGA is usually estimated from seismic hazard studies, but in cases where these studies are not available for class-A dams, PGA is estimated from acceleration maps or other simplified methods. This method can be used for designing against OBE and MCE.

Method 6 – Saragoni (1993) with PGA = A_0

This method evaluates k_h using equation (2) adopting the A_0, depending on the location of the TSF in the seismic zones of the NCh433 standard (see Figure 1a). The evaluation of the equation is a function of the PGA estimated at the site with simplified methods (usually without a formal seismic hazard analysis).

$$k_h = \begin{cases} 0.3\frac{A_0}{g} & PGA \leq 0.67g \\ 0.22\left(\frac{A_0}{g}\right)^{\frac{1}{3}} & PGA > 0.67g \end{cases} \tag{8}$$

Method 7 – Incremental method

This method begins by adopting a low value of k_h and calculating the FoS_{PS} of the dam downstream slope, using the limit equilibrium method. Then, the k_h is increased and the FoS_{PS} is recalculated. This procedure is repeated until achieving FoS_{PS}= 1.2, the minimum value required for pseudo-static analysis according to DS248. Finally, the horizontal seismic coefficient associated to FoS_{PS} = 1.2(k_h*) is compared with k_h values typically adopted in standard practice. If k_h* is lower than the values adopted in practice, the dam design is accepted. The lack of a sound rational criterion to compare k_h* makes this method highly subjective.

Method 8 – Bray et al. (2018)

Bray *et al.* (2018) proposed a simplified procedure to estimate seismic displacements of slopes subjected to interface and inslab earthquakes in subduction zones. The study builds on the theoretical framework of Bray and Travasarou (2007), considering a fully coupled model of a flexible one-dimensional soil column with nonlinear behavior and stick-slip behavior at the base. The parameters of the sliding mass that allow estimating the seismic displacement D_s (equation (9)) are the yield seismic coefficient of the sliding mass (k_y) and its fundamental period (T_s). The parameters related to the seismic hazard are the earthquake moment magnitude (M) and the spectral acceleration of the ground motion at a degraded period of the sliding mass, $T = 1.5T_s$, $S_a(1.5Ts)$.

$$\begin{aligned}\ln(D_s) &= a_1 - 3.353\ln\left(k_y\right) - 0.390\left[\ln\left(k_y\right)\right]^2 \\ &+ 0.538\ln\left(k_y\right)\ln\left[S_a\left(1.5T_s\right)\right] \\ &+ 3.060\ln\left[S_a\left(1.5T_s\right)\right] - 0.225\left\{\ln\left[S_a\left(1.5T_s\right)\right]\right\}^2 \\ &+ a_2T_s + a_3\left(T_s\right)^2 + 0.550M \pm \varepsilon\end{aligned} \tag{9}$$

The other parameters in the equation (9) are ε, a normally distributed random variable with zero mean and standard deviation = 0.73, and the constants a_1, a_2, and a_3, that depend on T_s (a_1 = -6.896, a_2 = 3.081 and a_3 = -0.803 for $T_s \geq 0.10$ s and a_1 = -5.864, a_2 = -9.421, and a_3 = 0 for $T_s < 0.10$ s). The k_y of the nonlinear, coupled deformable stick-slip sliding model is simply the friction coefficient at the model base whereas k_y of a sliding mass analyzed with the limit equilibrium method depends on the soil strength and the geometry of the mass. However, for practical applications it is assumed that both yield seismic coefficients are the same. From equation (9), the yield seismic coefficient can be derived if D_s is assumed as a tolerable seismic displacement

$$\begin{aligned}k_y &= \exp\left(\frac{-a+\sqrt{b}}{0.780}\right) \\ \text{where } a &= 3.353 - 0.538\ln\left[S_a\left(1.5T_s\right)\right] \\ b &= a^2 - 1.560\{\ln\left(D_s\right) - a_1 - 3.060\ln\left[S_a\left(1.5T_s\right)\right] \\ &+ 0.025\ln\left[S_a(1.5T_s)\right]^2 - a_2T_s - a_3(T_s)^2 - 0.550M - \varepsilon\}\end{aligned} \tag{10}$$

In the Chilean practice, the horizontal seismic coefficient is defined as $k_h = k_y$ for an arbitrary allowable seismic displacement (D_s), albeit k_h is associated to $FoS_{PS} \geq 1.2$.

Method 9 – Modified Saragoni

The modified Saragoni (1993) method defines an equation similar to equation (2), adapted for inslab earthquakes.

$$k_h = \begin{cases} 0.214\frac{PGA}{g} & PGA \leq 0.67g \\ 0.22\left(\frac{PGA}{2.51g}\right)^{\frac{1}{3}} & PGA > 0.67g \end{cases} \tag{11}$$

This method was considered by the same engineering firm for two class-C dams that are currently active. This equation was an attempt to consider the high PGAs expected for inslab earthquakes before the publication of Saragoni and Garrido (2022). However, the derivation of equation (11) is not explained in the stability analyses report.

Method 10 – Bray and Travasarou (2009)

Bray and Travasarou (2007) developed a simplified procedure to estimate seismic displacements of slopes subjected to shallow crustal earthquakes. The method follows the same principles than Bray's *et al.* (2018) method. The displacement prediction equation can be reworked to solve k_y as a function of D_s, T_s, S_a, and M (parameters defined before) (Bray and Travasarou, 2009)

$$\begin{aligned}k_y &= \exp\left(\frac{-a+\sqrt{b}}{0.665}\right) \\ \text{where } a &= 2.83 - 0.566\ln\left[S_a\left(1.5T_s\right)\right] \\ b &= a^2 - 1.33\{\ln\left(D_s\right) + 1.10 - 3.04\ln\left[S_a\left(1.5T_s\right)\right] \\ &+ 0.244\ln\left[S_a\left(1.5T_s\right)\right]^2 - 1.5T_s - 0.278(M-7) - \varepsilon\}\end{aligned} \tag{12}$$

Similar to the method of Bray *et al.* (2018), the horizontal seismic coefficient is defined as $k_h = k_y$ for an arbitrary allowable seismic displacement (D_s).

Method 11 – Seed (1979)

Seed (1979) recommended for design that k_h should depend on the earthquake magnitude for sites close to the

seismic source as shown in equation (13), provided that the deformations of the analyzed earth dam is acceptable for $FoS_{PS} \geq 1.15$ and crest accelerations lower than 0.75g.

$$k_h = \begin{cases} 0.10 & 6.5 \leq M < 8.5 \\ 0.15 & M \geq 8.5 \end{cases} \quad (13)$$

Chilean tailings dams database

The database developed in this study compiles information gathered from reports provided by Sernageomin; particularly from the TSFs database (Sernageomin, 2024), slope stability analyses, seismic hazard studies, dynamic analyses, Sernageomin's project approval resolutions, quarterly reports of TSFs operation and maintenance (E700 reports), and engineering reports. The database includes information collected from the most recent documents available of 125 TSFs constructed in Chile, including seismic coefficients (horizontals and verticals), dam height, seismic hazard information, and factors of safety. The database includes 73 active, 44 inactive, and 8 abandoned (*i.e.*, without current known owner) TSFs. The parameters considered in the database are listed in Table 2.

The database categorizes seismic coefficients, PGAs, earthquake mechanisms, as well as static and pseudo-static factors of safety according to the type of earthquake adopted in the design, either OBE or MCE. The definitions of these earthquakes are those from the D50 standard reviewed in the introduction.

Table 3 shows the number of dams designed for OBE and MCE. Out of the 125 analyzed dams, 51 considered k_h for OBE and MCE (k_{hOBE} and k_{hMCE}) and only 8 of these dams considered additionally vertical seismic coefficients for OBE and MCE (k_{vOBE} and k_{vMCE}). Thirty-three dams were designed based on the k_{hOBE}, and 41 dams were designed considering the k_{hMCE}. From this last group of dams, 23 considered that the MCE was equivalent to the OBE. It is worth noting that 101 dams disregarded k_v in their designs. Provided that some dams were designed for OBE and MCE, this study compiled 92 analyses for MCE and 84 analyses for the OBE, *i.e.* a total of 176 analyses.

Figure 1(a) shows the distribution of the 73 active and 52 non-active TSFs (44 inactive and 8 abandoned) throughout the Chilean territory, emphasizing the seismic zone of the Chilean standard NCh433. Four facilities locate in Zone 1, 19 in Zone 2, and 102 in Zone 3. Figure 1(b) classifies the dams according to the facility type (13 filtered, 52 embankments, 55 sand dams, 1 paste, and 4 pools) and construction method (70 downstream, 30 centerline, 12

Table 2: Parameters considered in the database

Parameter	Description
k_{hOBE}	Horizontal seismic coefficient for OBE (-)
k_{hMCE}	Horizontal seismic coefficient for MCE (-)
k_{vOBE}	Vertical seismic coefficient for OBE (-)
k_{vMCE}	Vertical seismic coefficient for MCE (-)
Method	Method for estimating the horizontal seismic coefficients (see Table 3)
Year	Year of the dam slope stability analysis
Height	Dam height according to design (m)
Volume	Impoundment volume according to design ($10^6 \cdot m^3$)
PGA_{OBE}	Peak Ground Acceleration for OBE (g)
PGA_{MCE}	Peak Ground Acceleration for MCE (g)
Class	Facility class according to D50 (A, B and C)
Seismic zone	Seismic zone according to NCh433 (1, 2, and 3)
OBE mechanism	Mechanism of OBE defined by seismic hazard study (Inslab, interface, and shallow crustal)
MCE mechanism	Mechanism of MCE defined by seismic hazard study (Inslab, interface, and shallow crustal)
FoS_{OBE}	Pseudo-static factor of safety for OBE (-)
FoS_{MCE}	Pseudo-static factor of safety for MCE (-)
FoS_{ST}	Static factor of safety (-)
Status	Current status of the TSF (active, inactive, and abandoned)
Type	Type of tailings facility or dam (embankment, sand dam, filtered, paste, and pool)
Constructive method	Dam or facility constructive method (downstream, centerline, terrace, upstream, and other methods)

Table 3: Number of analyzed tailings dams for OBE and MCE

	Vertical seismic coefficients				
Horizontal seismic coefficients	k_{vOBE} and k_{vMCE}	k_{vMCE}	k_{vOBE}	Without k_v	Total
k_{hOBE} and k_{hMCE} (1)	8	2	0	41	51
k_{hOBE}	0	0	2	31	33
$k_{hOBE} = k_{hMCE}$	0	3	0	20	23
k_{hMCE}	0	9	0	9	18
Total	8	14	2	101	125

Note (1): Same method for estimating k_{hOBE} and k_{hMCE}

terraces, 6 upstream, and 7 other methods). Sand dams are built using the coarser fraction of the tailings, whereas embankment dams are earth fills built with borrowed materials. Tailings pools are impoundments that benefit from natural depressions or excavations and paste facilities can be conventional dams where the tailings are dewatered and stockpiled to minimize the occupied surface area. The downstream, centerline, and upstream construction methods were used for sand dams, embankments, and paste facilities. Filtered tailings impoundments are formed into compacted terraces that are self-supported without a buttress. Combinations of construction methods were grouped into "other".

Figure 1(b) shows that the downstream construction method has been the most adopted given its proper seismic stability and that a limited number of dams were designed following the upstream construction method, which was banned by the D86, except in cases explicitly authorized by the Director of the State Mining Service (Ministerio de Minería, 1970). These upstream dams are currently inactive.

Figure 2(a) shows the number of TSF in each region of Chile, considering their status (active, inactive, and abandoned) and their classification according to the D50 (class A, B, and C). Figure 2(b) shows the number of dams according to their heights. The compiled dams range from 4 to 310 m height, but most of the dams are between 4 and 15 m height.

The database compiled herein is a representative subset of the 791 TSFs reported by Sernageomin (2024). The active dams analyzed in this database represent about 55% of the currently active TSFs. In addition, as shown in the inset of Figure 2(b), the 125 analyzed facilities account for nearly 72% of the total authorized storage tailings volume in Chile.

a)

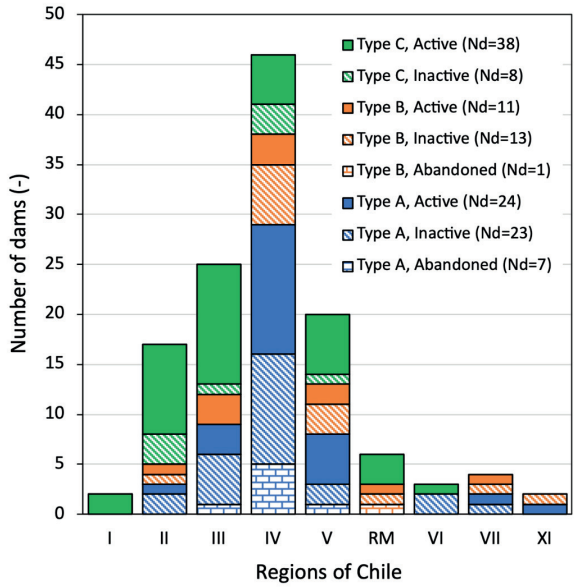

b)

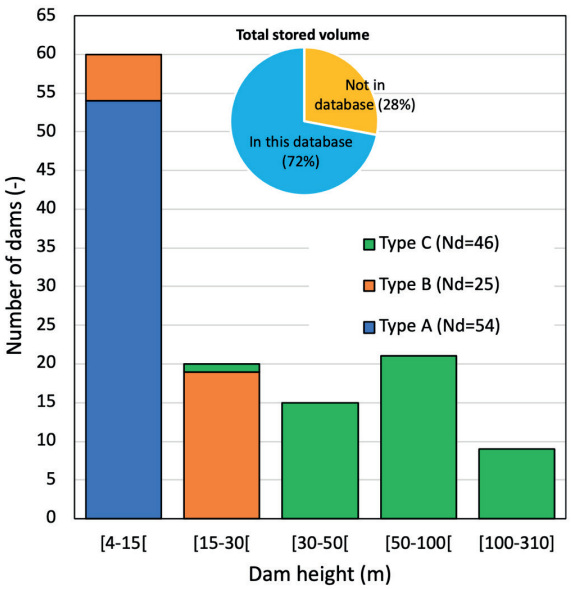

Figure 2: a) Number of dams by region (shown in Figure 1), considering the current TSFs status (active, inactive, and abandoned) and classification type (A, B, and C), according to the D50. b) Heights and D50 classification type of the 125 analyzed tailings dams.

Database analyses

Table 4 shows the number of TSFs that adopted the different reviewed methods to estimate the k_h. As mentioned above, the database considers 84 cases for the OBE (Na = 51+33 cases in Table 3) and 92 cases for the MCE (Na = 51+23+18 cases in Table 3).

Figure 3 shows the horizontal seismic coefficients associated with the different calculation methods for the OBE (Figure 3(a)) and the MCE (Figure 3(b)) in box-and-whisker diagrams, displaying the minimum and maximum values, the median, as well as the first and third quartiles. The figure also shows the individual k_h values on top of the box-and-whisker diagrams. In some instances, outlier data points plot outside the whiskers.

The most adopted method is that of Saragoni (1993, Method 1) in 54 of the 125 dams (*i.e.*, 43.2% of the cases see Table 4) . This method was defined from quay walls failed during Japanese earthquakes and was not specifically defined for tailings dams. However, it has been adopted in several designs, mainly in large dams (31 class-C dams). The medians of the 43 and 49 values adopted for the OBE

Table 4: Number of dams designed with different methods for estimating the horizontal seismic coefficient

Method	# Dams	%	Type A		Type B		Type C	
			Active	Non-active	Active	Non-active	Active	Non-active
1. Saragoni (1993)	54	43.2	10	3	6	4	26	5
2. D86 (1970)	18	14.4	1	13		3		1
3. Guidelines DS248 (2016)	15	12.0	7	4	2		2	
4. NCh433 (1996)	8	6.4	2	5	1			
5. Fraction of PGA	7	5.6	2	2		1	1	1
6. Saragoni (1993) with PGA=A_0 (NCh433,1996)	5	4.0	1		1	2	1	
7. Incremental method	3	2.4				3		
8. Bray *et al.* (2018)	2	1.6		1			1	
9. Modified Saragoni	2	1.6					2	
10. Bray and Travasarou (2009)	1	0.8					1	
11. Seed (1979)	1	0.8		1				
Unspecified	9	7.2	1	1	1	1	4	1
Total	125	100	24	30	11	14	38	8

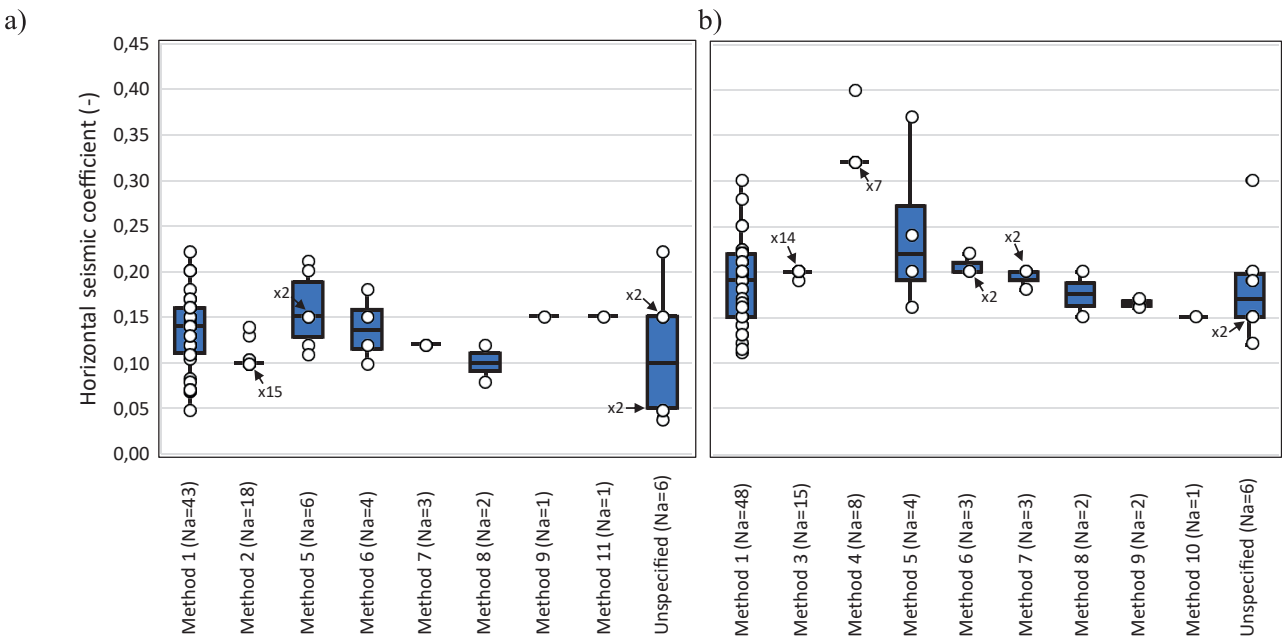

Figure 3: Distribution of horizontal seismic coefficients estimated from methods in Table 4, considering: (a) OBE in 84 analyses and (b) MCE in 92 analyses.

and MCE with this method are k_{hOBE} = 0.134 and k_{hMCE} = 0.186, respectively.

The second most adopted method is that of the D86 (1970, Method 2), a valid method before the enactment of the DS248 in 2007. The database recognizes two small dams designed after 2007 that considered this method. Out of the 18 dams designed for OBE using this method, 14 were small dams (class A, see Table 4). Figure 3 shows that 15 of these dams considered k_{hOBE} = 0.1, meaning the number of inhabitants within the critical zone determined by the

hazardous distance was $N = 0$. This condition could have changed over time.

The third most adopted method is that of the Guidelines DS248 (2016, Method 3) in the design of 15 dams for MCEs. These dams are shorter than 30 m and 11 of them classify as class-A dams (see Table 4), as intended by the Sernageomin. However, there are two class-B and two class-C active dams that considered this method in their designs. These dams where located in seismic zone 3, then $k_h = 0.2$ was adopted, except in one case where k_h was reduced to $k_h = 0.19$.

The design of the eight class-A and class-B dams that considered Method 4 is among the most conservative since the k_h estimated with this method for MCE exceeds $k_{hMCE} = 0.32$ (Figure 3(b)). These are dams shorter than 15 m height.

Method 5 was adopted in the design of six class-A, -B and -C tailings dams for OBE (Figure 3(a)). Three of these dams were also verified for MCEs (an additional dam was verified only for MCE). Like Saragoni's method, k_h estimated with Method 5 can considerably vary provided the variability of PGA for MCE (Figure 3(b)).

Five class-A, - B and -C dams were designed considering Method 6. Figure 3 shows that the range of k_h values is much narrower than Method 1 since only three values of A_0 are considered.

The Method 7 was adopted in three class-B dams designs for OBE and MCE and Method 9 was adopted in two class-C dams, which exceed 160 m height. Both methods provided narrow ranges of k_h values.

Performance-based Methods 8 and 10 that considered the allowable dam displacements were used on three dams, one class-A and two class-C. Figure 3 shows that k_h values are lower than 0.12 for OBE and lower than 0.2 for MCE.

Finally, a current inactive class-A TSF estimated k_h using the Method 11 for a large magnitude earthquake ($k_h = 0.15$). No information regarding the k_h estimation method was found for nine dams. The values range from 0.04 to 0.22 for OBE and from 0.12 to 0.30 for MCE.

Seismic coefficients and PGA through time

Figure 4 shows the values of k_h and PGA over time, from 1983 to 2022, based on the year of elaboration of the seismic stability analysis reports. k_h slightly varied in the 80's, 90's and early 00's since the D86 required the use of equation (3) for the calculation of k_h. No estimation of PGA was required at that time. Most of these cases correspond to dams of less than 30 m height. After 2002, k_h began to increase, exceeding $k_h = 0.3$ in 2009. Saragoni's (1993) method is used for the first time in this database in 2005, 12 years after the article was published.

From 2020, the adopted k_h values were lower than 0.22, contrasting with the larger variability of previous years. This variability is related to a large number of projects developed in recent years and the freedom to estimate k_h for operational and closure conditions.

Figure 4(b) also shows the PGA considered in the dams design. The first hazard studies in the database date from 2003, prior to which the PGA was not estimated or simply not reported. Since 2014, PGA_{MCE} values began to exceed 1.0g, which may be related to technological advancements in accelerographs, such as improved dynamic range and higher sampling rates, which has enabled the recording of larger PGAs in recent earthquakes.

Relationship between k_h and PGA

Figure 5 relates the horizontal seismic coefficient to the peak ground acceleration estimated from seismic hazard studies. Cases lacking an estimation of PGA were grouped at PGA = 0. These later cases generally correspond to projects that do not have a specific seismic hazard study and adopted Methods 3, 4, 7 y 11.

The most repeated k_h values for OBE and MCE are in the ranges [0.1, 0.15[and [0.2, 0.25[, respectively. The figure also shows the relationship between k_h and PGA defined by equation (2), according to Saragoni (1993). The cases that adopted this method were plotted in blue symbols. Some points deviate from the curve since the values obtained using equation (2) where rounded or approximated. Six cases with known PGA that considered other methods adopted k_h lower than values predicted by Method 1. Two of these cases did not specify the calculation method, two cases considered performance-based methods (Method 8 and 10), and two cases considered the Method 9. The four later cases are active class-C TSFs.

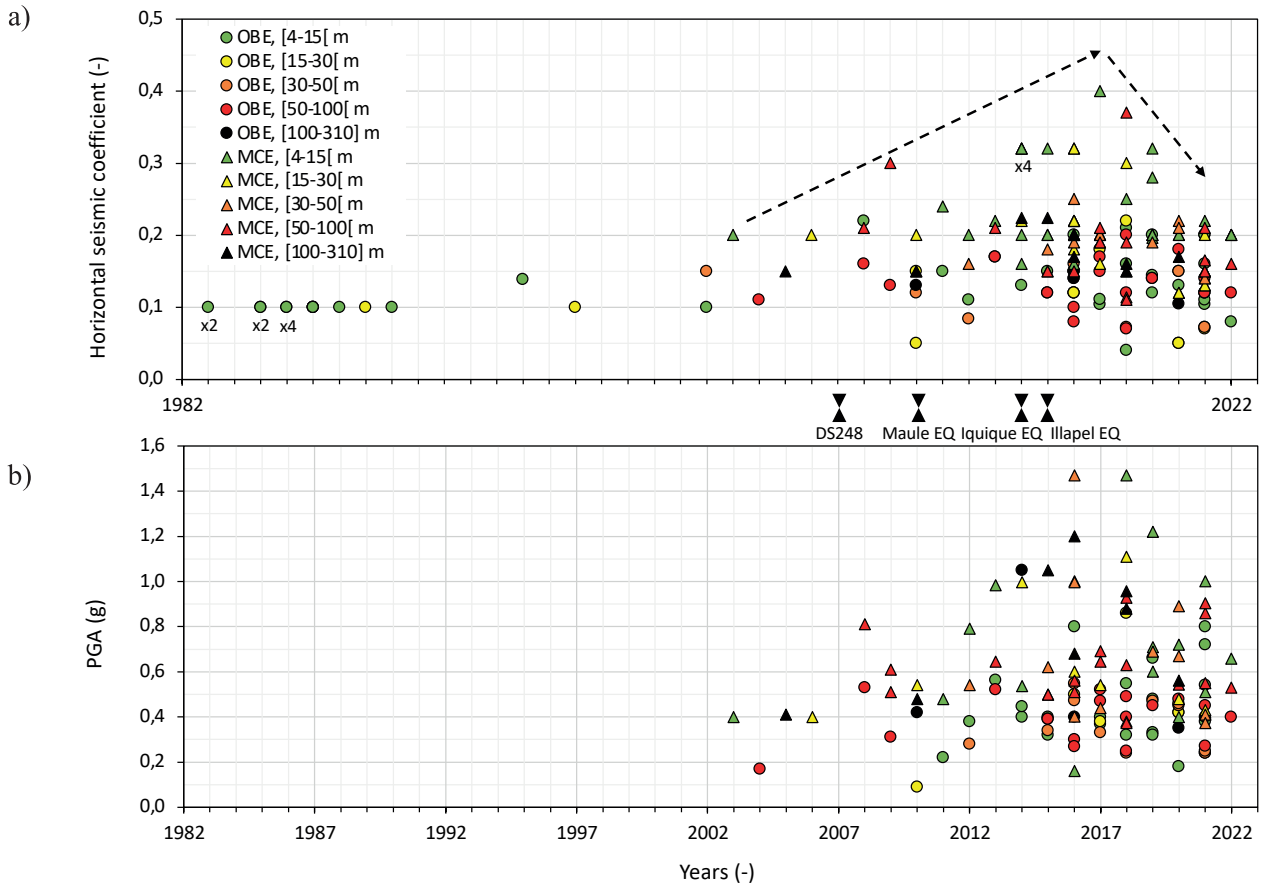

Figure 4: (a) Horizontal seismic coefficients and (b) peak ground accelerations (PGA) as a function of the year of the stability analyses for the 125 TSFs. Cases are discretized by dam height. The enactment of the DS248 in 2007, as well as the megathrust 2010 M_w 8.8 Maule, 2014 M_w 8.2 Iquique and 2015 M_w 8.3 Illapel earthquakes are included as references

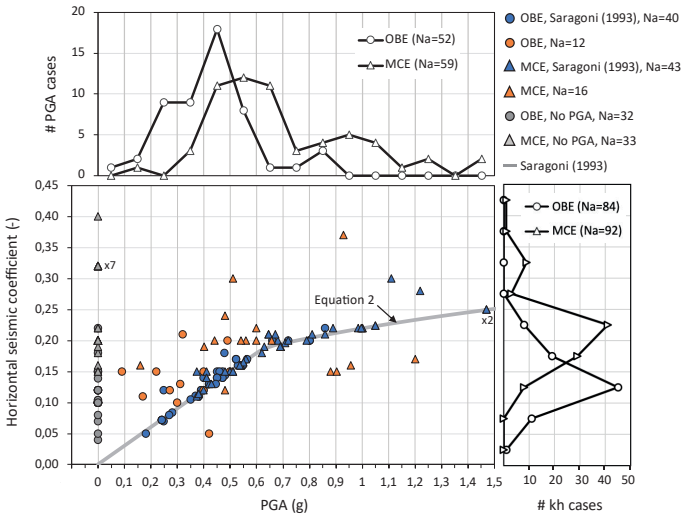

Figure 5: Horizontal seismic coefficient as a function of PGA for the 125 analyzed TSFs. 92 analyses for MCE and 84 analyses for OBE are considered (Na = 176)

Two analyses that considered Method 1 and PGAs larger than 1.1g plot above the relationship proposed by equation (2). These larger values were adopted to provide safer designs considering the occurrence of MCEs.

Relationship between k_h and the tailings dams heights

Figure 6 shows the relationship between k_h and the maximum height of the analyzed dams. Note that the two dams exceeding 200 m in height shown in the figure correspond to projected, not actual heights. Dams taller than 70 m are active (blue symbols) and their k_h values range between 0.105 and 0.17 for OBE and from 0.15 to 0.224 for the MCE. Dams taller than 100 m were designed with $k_{hMCE} \leq 0.224$ for MCE. In contrast, for dams smaller than 15 m height, many of which are non-active TSF, a wider range of k_h values was adopted, between 0.04 and 0.22 for OBE and between 0.12 and 0.4 for MCE. As highlighted in the figure. Method 4 was exclusively adopted in small TSFs, resulting in large k_h values.

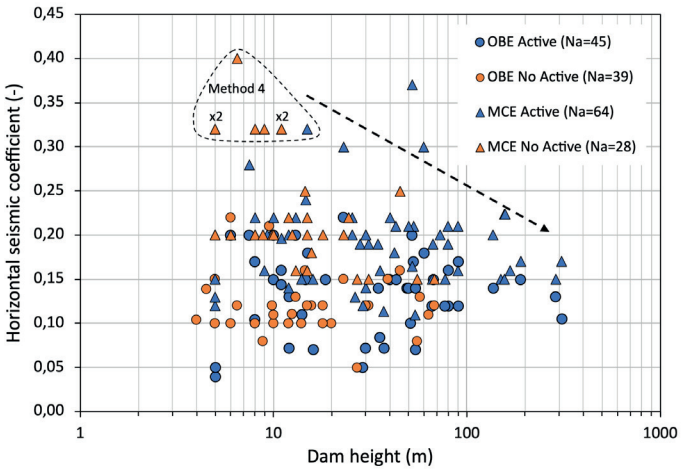

Figure 6: Horizontal seismic coefficient as a function of dam height for the 125 analyzed TSFs. 92 analyses for MCE and 84 analyses for OBE are considered (Na = 176)

Vertical seismic coefficients

Figure 7 shows the relationship between the horizontal and vertical seismic coefficients available for 32 analyses in 24 dams. The vertical seismic coefficient (k_v) is usually calculated as a fraction of k_h and is bounded between 1/3 k_h and 2/3 k_h for OBE and MCE. Although 10 analyses considered k_v for OBE and 22 analyses considered k_v for MCE, only 24 dams out of the 125 studied TSFs (19.2%) considered the effect of the vertical seismic coefficient in addition to the horizontal coefficient. We confirmed that the adoption of the vertical seismic coefficient has not been characteristic of any type of dam or controlling earthquake mechanism.

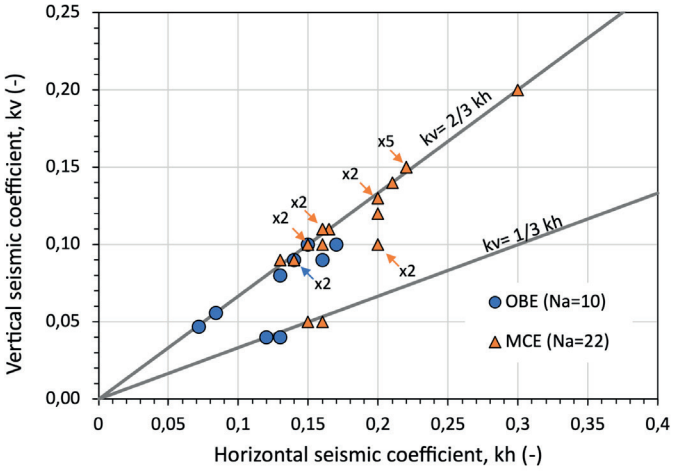

Figure 7: Horizontal and vertical seismic coefficients for Nd = 24. Arrows highlight OBE and MCE values associated to more than one case

Relationship between k_h, FoS, PGA and tailings dams heights

The factors of safety documented in the analyzed reports were calculated using different geotechnical software, such as GeoStudio, Slide2, Utexas4, and Slope Stability Calculator. In addition, six instances used alternative approaches, such as graphical or simplified methods.

Figure 8 shows the 125 analyzed tailings dams, each connected with a vertical line in the four panels showing the dam height, the static and pseudo-static factors of safety, FoS_{ST} and FoS_{PS}, as well as the k_h and the PGA for OBE and MCE. The figure is divided into five sectors.

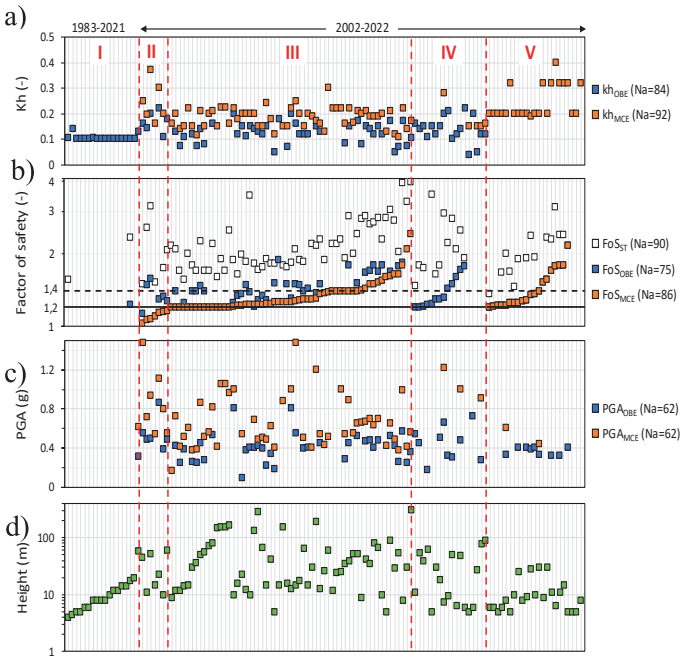

Figure 8: a) Horizontal seismic coefficients, b) static and pseudo-static factors of safety, c) PGAs for OBE and MCE, and d) dam heights for the 125 analyzed TSFs. Each vertical line corresponds to one dam. The sectors I, II, III, IV, and V are described in the text

The first sector (I) clusters 18 dams that estimated k_h using the Decree No. 86 (Method 2) from 1983 to 2021 sorted by the dams' heights. Nearly in all cases, $k_{hOBE} = 0.1$ since equation (3) was evaluated with $N = 0$. The heights of these dams do not exceed 58 m.

The second sector (II) groups seven dams designed from 2012 to 2020 with $1.0 < FoS_{MCE} < 1.2$. Dam heights in this sector range from 10 to 60 m. Class-A and -B dams in this

sector do not comply the minimum factor of safety FoS_{PS} = 1.2 required by the D50.

The third sector (III) corresponds to 59 dams designed from 2005 to 2022 with $FoS_{MCE} \geq 1.2$ sorted from the lowest to the highest FoS_{MCE} values. Dam heights in this sector range from 5 to 310 m.

The fourth sector (IV) corresponds to 18 dams designed between 2002 and 2022, whose FoS_{MCE} was not found (or not computed). In this case, dams were sorted from the lowest to the highest $FoS_{OBE,}$ when available. Dam heights in this sector range from 5 to 90 m.

The last sector (V) corresponds to 23 dams that considered $k_{hOBE} = k_{hMCE}$ and adopted Methods 3 and 4 for their estimation. It is assumed that $FoS_{MCE} = FoS_{OBE}$ and dams were sorted from the lowest to the highest FoS_{MCE}, when available. Their designs were performed between 2006 and 2022. Dams in this sector have the highest k_h values and their heights range from 5 to 30 m. Most of these dams do not have seismic hazard studies to estimate PGA.

Figure 9 shows the relationship between static and pseudo-static factors of safety for OBE and MCE, FoS_{OBE} and FoS_{MCE}, respectively. Most cases comply with the requirements of Chilean regulations, $FoS_{PS} \geq 1.2$ and $FoS_{ST} \geq 1.4$.

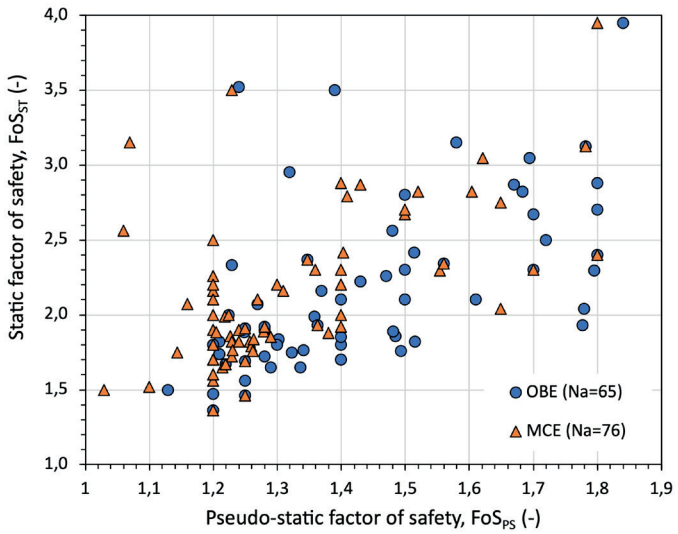

Figure 9: Pseudo-static and static factors of safety for Na = 141.

Spatial distribution of k_h and PGA

Figure 10 shows the spatial distribution of k_h and PGA for OBE and MCE in the Chilean territory. There is no relationship between the location of the TSFs and the value of the adopted seismic coefficient, except for the dams that adopted Methods 3, 4, and 6 that depend on A_0. Moreover, PGA_{OBE} and PGA_{MCE} are not spatially correlated either.

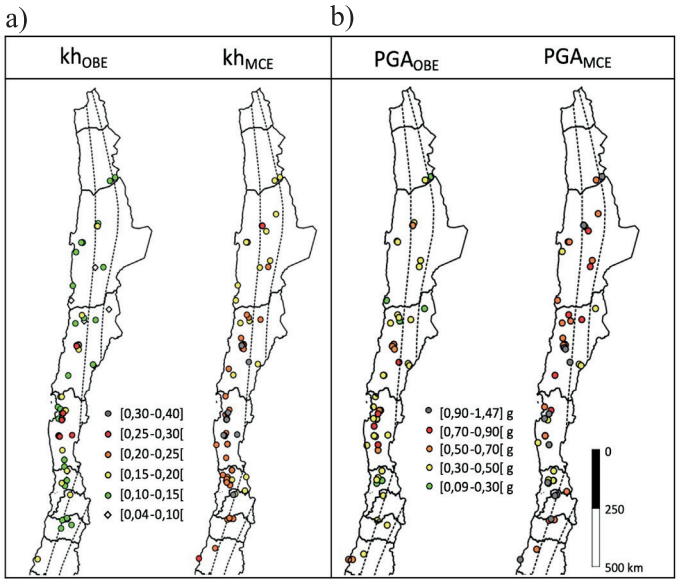

Figure 10: Spatial distribution of: (a) horizontal seismic coefficients for Na = 176 and b) PGA for Na = 124 available analyses, considering OBE and MCE

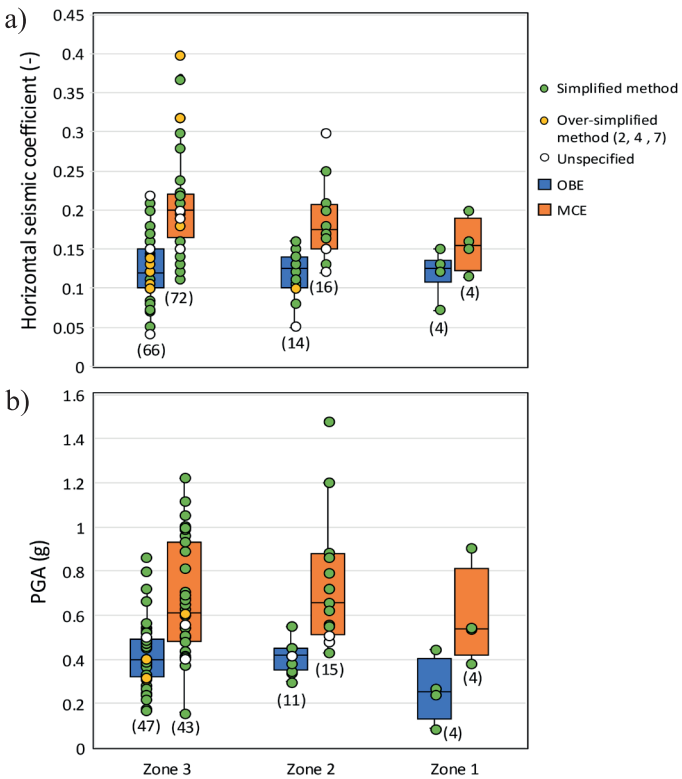

Figure 11: Distribution of: (a) horizontal seismic coefficients for Na = 176 and (b) PGA for Na = 124, adopted in the seismic zones of the NCh433 standard

Figure 11 shows the values of k_h and PGA in each of the seismic zones defined in the seismic design standard NCh433. In average, PGA and k_h for MCE and OBE tend to be larger in zones 3 and 2, compared to zone 1. On the other hand, the largest k_h values are found in the seismic zone 3, having the highest variability of all, with k_h values ranging from 0.04 to 0.23 for the OBE and from 0.11 to 0.40 for the MCE. No systematic trend was found regarding the type of method adopted in the k_h estimation.

Figure 12 shows the values of k_h and PGA for various types of earthquake mechanisms considered in the design (interface, inslab, and shallow crustal). Most of the designs were controlled by inslab earthquakes, but slightly larger k_h were adopted for interface earthquakes.

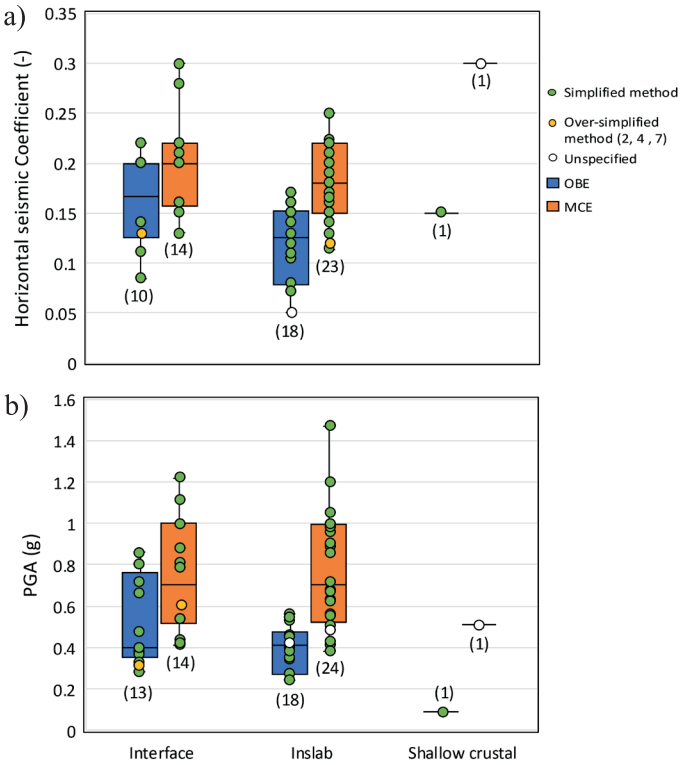

Figure 12: Distribution of: (a) horizontal seismic coefficients for Na = 67 and (b) PGA for Na = 71, considered for different earthquake mechanisms

Discussion

Methods for estimating k_h

The database review reveals that 11 different approaches have been adopted to estimate k_h in the design process of tailings dams in Chile from 1983 to 2022. Table 5 compares the methods, highlighting their most significant advantages and limitations. Three of these methods depend exclusively on PGA, disregarding the dam geometry, the geotechnical properties, and the location of the potential sliding mass. Nonetheless, several dams have been designed with Saragoni's (1993) method and have withstood strong megathrust earthquakes.

As pointed out by Seed and Martin (1966), taller dams with longer fundamental periods, larger sliding masses extending through the full dam height, and dams built with lower shear wave velocity materials can be designed with smaller horizontal seismic coefficients. If these methods were adopted in engineering practice, we recommend to estimating the PGA from seismic hazard analyses, accounting for local site and topographic amplification effects, and not from simplified methods. Although PGA is easier to estimate, other intensity measures, such as PGV and Arias Intensity, have demonstrated to be better correlated with slopes seismic displacements (*e.g.*, Cho and Rathje, 2022). However, to the best of the authors knowledge, no methods for estimating k_h have been developed based on other intensity measures different from PGA.

As for the performance-based methods, such as Bray *et al.* (2018, Method 8) and Bray and Travasarou (2009, Method 10), the local engineering practice adopts k_h as the yield seismic coefficient (k_y), which is conceptually erroneous since the Chilean regulation enforce a minimum pseudo-static factor of safety of 1.2 (read the details in the introduction). Although these methods account for parameters related to the sliding mass stiffness and the input ground motion (intensity and duration), the selection of the allowable seismic displacement is usually overestimated in the engineering practice, resulting in horizontal seismic coefficients lower than those estimated with PGA-based methods for equivalent seismic hazard levels. Since these methods begin to be adopted since 2018, no large earthquakes have affected the dams designed with these methods.

The method of the Decree No. 86 (1970, Method 2) is a risk-based one that depends on the number of inhabitants within a critical zone in case of a catastrophic dam failure (*i.e.*, k_h increases with the potential population at risk). Most of the tailings dams that considered this method assumed few people or no population settled downstream within the

Table 5: Characteristics of methods for estimating seismic coefficients in Chilean tailings dams

Method	Years of use	Advantages	Limitations
1. Saragoni (1993)	2005-2022	Evaluation of k_h only requires the PGA at the site, which can be readily estimated from seismic hazard analyses.	1. Formulated from retaining walls under limit equilibrium condition in harbor facilities subjected to interface earthquakes. 2. The method does not consider the geometry and dynamic properties of the dam. 3. Displacements of the dam are disregarded.
2. Decree No. 86 (1970)	1983-2021	Evaluation of k_h only requires number of inhabitants within a critical zone determined by the hazardous distance after the tailing's facility closure, following a consequence classification approach.	1. The method does not consider the geometry and dynamic properties of the dam. 2. It estimates a low k_h value ($k_h = 0.1$) when fewer than 25 inhabitants are near the hazardous area. k_h increases slowly with the number of inhabitants.
3. Guidelines DS248 (2016)	2006-2022	Evaluation of k_h only requires the location of the TSF in the Chilean territory to define the seismic zone, according to NCh433 (see Figure 1).	1. Although the method was proposed solely for small-scale mining, it has been adopted in the design of large TSFs. 2. The method may underpredict k_h in TSFs with large seismic hazard (large PGA).
4. NCh433 (1996)	2014-2019	Not recommended	1. Flawed method formulation since k_h is estimated as the maximum seismic coefficient used to calculate the basal shear stress in building design. 2. The method predicts very high k_h values compared to other methods.
5. Fraction of PGA	2004-2022	Similar to advantages of Method 1.	1. The α factor depends on the designer expert judgment, which can lead to high k_h variability.
6. Saragoni (1993) with PGA = A_0 (NCh433,1996)	2015-2021	Not recommended	1. Estimated PGA (= A_0) can be underpredicted in TSFs with large seismic hazard (PGA > 0.4g).
7. Incremental method	2016	Not recommended	1. It is a verification method rather than a k_h estimation method; thus, it does not consider any physical input parameter. Large variability can be reached depending on the static stability of the dam.
8. Bray *et al.* (2018)	2021-2022	Considers more physical parameters compared to the other methods, such as the seismic hazard spectrum, the period of the sliding mass, the earthquake magnitude, and the allowable seismic displacement.	1. Considers that $k_h = k_y$, which is not valid for the minimum pseudo-static factor of safety required by Chilean standards ($FoS_{PS} > 1.2$ as described in the introduction). 2. Usually, the allowable seismic displacements imposed by designers are larger than the values compatible with the method, leading to low k_h values compared with other methods. 3. The method disregards volumetric strain.
9. Saragoni (1993) modified	2016-2018	Similar to advantages of Method 1.	1. Since the formulation accounts for inslab earthquakes with larger PGA than interface earthquakes, it provides low k_h values compared to other methods.
10. Bray and Travasarou (2009)	2018	Similar to advantages of Method 8.	1. Similar to limitations of Method 8. 2. The method was formulated for shallow crustal earthquakes, not for interface and inslab earthquakes.
11. Seed (1979)	2016	Straightforward use	1. Empirical values not specifically defined for Chilean earthquakes and dams.

critical zone, which results in $k_h \sim 0.1$, a value that can be considered low for a dam located in a high seismic hazard area. Moreover, the downstream population can increase over time, increasing the seismic risk in case of earthquake induced failure. For this reason, and given that the method neglects both dam-specific characteristics and seismic demand, its use is not recommended. Nonetheless, most of the dams that considered this approach were designed before 2017 and are currently inactive. Their physical stability may have improved with time since most of the stored water evaporated or seeped out of the facility.

Methods based on A_0 depend exclusively on the TSF location in the Chilean territory, assuming the seismic hazard of the coastal zone 3 is larger than the rest. This may be a good estimate when thrust earthquakes are the controlling mechanism for OBE and MCE, but it may be non-conservative if the controlling earthquake mechanism is inslab. From these A_0-based methods, Method 4 is the one that estimate the largest k_h whereas Methods 3 and 6 have predicted similar k_h values.

Relationship between k_{hMCE} and k_{hOBE}

Figure 13 shows the relationship between k_{hMCE} and k_{hOBE} in 51 TSFs (15 class-A, 10 class-B, and 26 class-C). The mean trend between both horizontal seismic coefficients can be approximated by

$$k_{hMCE} = 0.08 + 0.9k_{hOBE} \quad (14)$$

Figure 13 also shows that, disregarding outliers, the data can be bounded by equation (14) +/- 0.04.

Seismic performance of tailings dams

The seismic performance evaluation of tailings dams requires adequate information, such as records of vertical and horizontal displacements in different parts of the dam after an earthquake to verify the design intend adequacy. This detailed information is not available in this study. However, we identified a subset of 52 TSFs subjected to large megathrust earthquakes that did not suffer considerable damage and continued operating after the earthquakes.

The number of analyzed dams for each earthquake, considering OBE and MCE, are shown in Table 6. The earthquakes analyzed in this section are listed in Table 7, including their main characteristics. These dams were constructed with several methods and 21 of them were subjected to more than one earthquake. Note that earthquakes may have occurred at a dam construction stage different from the design condition. These dams did not suffer considerable damage during the analyzed earthquakes which somehow validates their seismic design. We understand that more comprehensive analyses are required to confirm the contribution of the pseudo-static analysis in the design process, but we also believe that this analysis can be a starting point for that validation process.

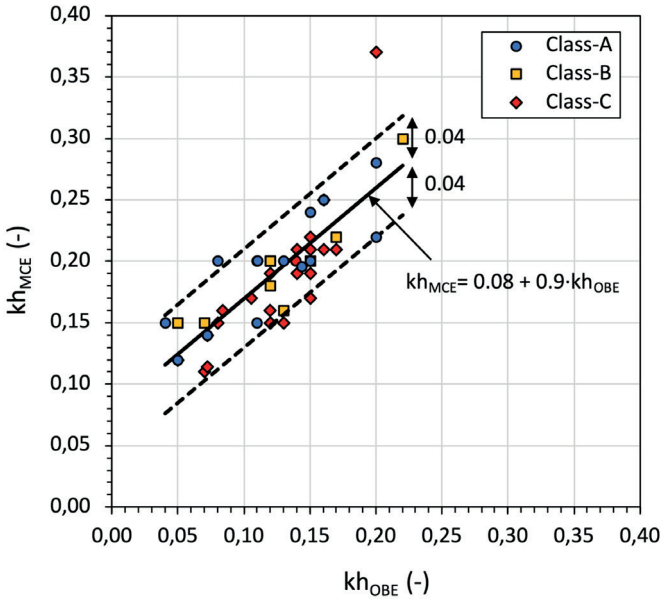

Figure 13: Relationship between k_{hMCE} and k_{hOBE} in 15 class-A, 10 class-B, and 26 class-C TSFs.

Table 6: Number of analyzed dams for OBE and MCE

Earthquake	# Dams	Cases for OBE	Cases for MCE
Antofagasta 1995	2	2	2
Punitaqui 1997	8	8	0
Tarapacá 2005	1	1	1
Tocopilla 2007	4	3	3
Maule 2010	18	12	14
Illapel 2015	40	29	22

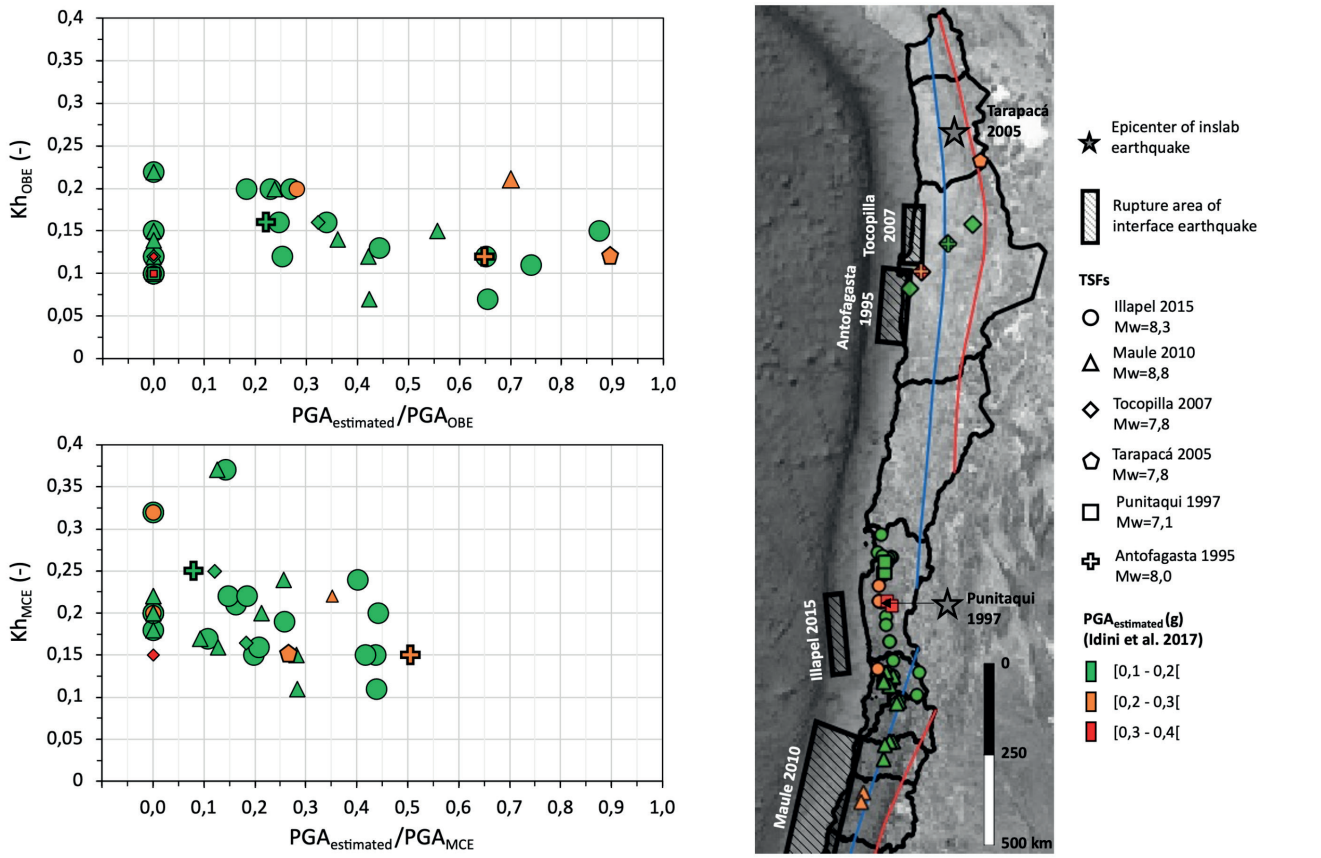

Figure 14: Fifty-two TSFs subjected to large earthquakes in Chile. Rupture areas of interface earthquakes and epicenters of inslab earthquakes were adopted from Idini *et al.* (2017). The mean PGA at the TSF sites were estimated using Idini *et al.* (2017) ground motion model, assuming rock outcrop conditions. Horizontal seismic coefficients for: a) OBE in Na = 56 and b) MCE in Na = 42

Figure 14 shows the location of these TSFs, along with the rupture areas of interface earthquakes and epicenters of inslab earthquakes, according to Idini *et al.* (2017). Figure 14(a) shows k_{hOBE} considered in 56 cases for these earthquakes as a function of the mean PGA estimated using the Idini *et al.* (2017) ground motion model for hard rock site condition ($PGA_{estimated}$) normalized by the PGA adopted for the OBE in the design (PGA_{OBE}). The ground motion model was evaluated at the TSFs sites as a function of the type of earthquake (inslab or interface), the distance from the site to the rupture area, the earthquake magnitude, and the focal depth. Likewise, Figure 14(b) shows k_{hMCE} considered in 42 cases for the analyzed earthquakes as a function of $PGA_{estimated}$ normalized by the PGA considered for MCE in the design (PGA_{MCE}). Values grouped at $PGA_{estimated}/PGA_{OBE} = PGA_{estimated}/PGA_{MCE} = 0$ in Figures 14(a) and 14(b) are dams without information about the PGA adopted in the design. The estimated PGAs are more likely comparable to the design values for OBE, in which case k_{hOBE} range from 0.07 to 0.22.

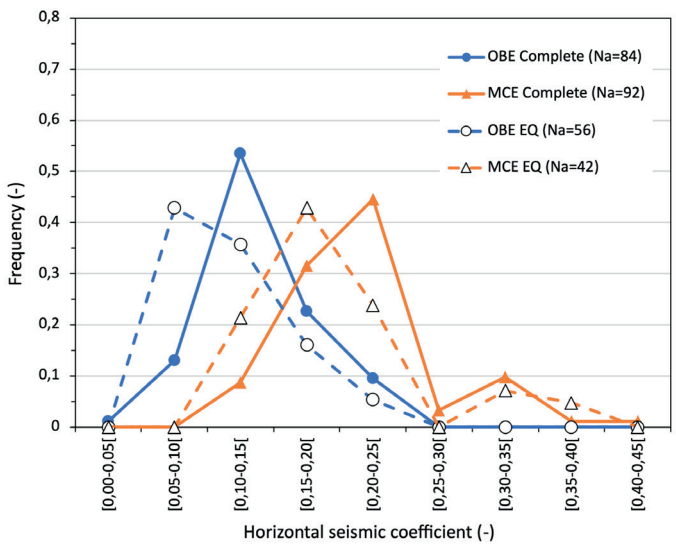

Figure 15: Distributions of k_{hOBE} and k_{hMCE} of the complete database and TSFs affected by large earthquakes (EQ) in Figure 14

Figure 15 compares the distribution of values of k_{hOBE} and k_{hMCE} of the complete database and that of k_h values adopted in the design of dams subjected to major earthquakes. The

Table 7: Analyzed earthquakes and their characteristics

Earthquake	Magnitude	Type	Latitude(1) (º)	Longitude(1) (º)	Rupture length(2) (km)	Rupture width(2) (km)	Strike(2) (º)	Dip(2) (º)
Antofagasta 1995	8.0	Interface	-25.00	-71.15	185	80	6	22
Punitaqui 1997	7.1	Inslab	-30.77	-71.22	N/A	N/A	N/A	N/A
Tarapacá 2005	7.8	Inslab	-19.93	-69.21	N/A	N/A	N/A	N/A
Tocopilla 2007	7.8	Interface	-23.25	-70.50	145	55	2	20
Maule 2010	8.8	Interface	-37.8	-74.45	500	150	19	18
Illapel 2015	8.3	Interface	-32.5	-72.5	200	50	4	19

(1) Latitude and longitude refer to the coordinates of the south-west vertex of the rectangular rupture plane associated to interface earthquakes (1) according to Idini *et al.* (2017). In the case of inslab earthquakes, the values correspond to the earthquake epicenter.
(2)Values of the rupture plane adopted from Idini *et al.* (2017) for interface earthquakes
(3) N/A: Not applicable

distributions are similar with k_{hOBE} ranging between 0.1 and 0.2 and k_{hMCE} ranging between 0.15 and 0.25. These values seem adequate for the seismic design of tailings dams in the Chilean subduction zone given the favorable seismic performance of the dams reported herein.

Conclusions and recommendations

The compiled database of 125 tailings dams, spanning 73 active and 52 non-active facilities, includes sand dams, embankments, filtered deposits, paste deposits, and tailing pools, being a representative subset of the facilities reported in the 2024 Sernageomin database. Eleven methods were used to estimate k_h, many of which only consider the seismic hazard through the PGA or A_0, disregarding the geometry and the material properties of the dams. The main adopted method was that of Saragoni's (1993) in 43.2% of the analyzed cases since 2005. The k_h defined with this method (equation (2)) can be considered as a lower bound of the analyzed data when PGA is available. The method was defined for interface earthquakes and can result in large k_h values for PGA exceeding 1g, particularly when inslab earthquakes are considered in the design. The k_{hOBE} ranged from 0.04 to 0.22 and the k_{hMCE} from 0.11 to 0.4 with a trend to decrease the k_h with the dam height. Most of the larger k_h compiled in this database were derived using methods that are not recommended in the present study. No trend in the k_h values was found regarding the location of the dams with respect to the seismic zones and the design earthquake mechanism.

Based on the analyses shown in this study, including the seismic performance of several dams, k_{hOBE} ranging from 0.1 to 0.2 and k_{hMCE} ranging from 0.15 to 0.25 seem adequate values for preliminary pseudo-static slope stability evaluations, depending on the seismic hazard level and the characteristics of the dam. We recommend that Methods 4, 6, and 7 are no longer considered in the future design of TSFs for the reasons explained in Table 5.

Only 24 of the 125 analyzed TSFs considered in their design the effect of the vertical ground motion, in addition to the horizontal motion. This is attributed to the absence of k_v requirements in the regulation. The adopted k_v values ranged from $1/3k_h$ to $2/3k_h$.

TSFs that complied with current Chilean regulations have not suffered catastrophic failures during the last megathrust earthquakes analyzed in the present study. We encourage mining companies to share information about the monitored seismic behavior of their facilities to compare their performance with the design intend. Qualitative and quantitative information is valuable to confirm the findings of this study. Advancing in the adequate estimate of k_h will allow to improve the confidence in the use of a simple stability assessment tool that complements numerical deformation analyses in the design of safe geotechnical structures.

References

Bowker, L.N. and Chambers, D.M. (2015). The risk, public liability and economics of tailings storage facility failures. *Earthwork Act* **24**, 1-56

Bray, J.D. and Travasarou, T. (2009). Pseudostatic coefficient for use in simplified seismic slope stability evaluation. *Journal of Geotechnical and Geoenvironmental Engineering* **135**(9), 1336-1340

Bray, J.D. and Travasarou, T. (2007). Simplified procedure for estimating earthquake induced deviatoric slope displacements. *Journal of Geotechnical and Geoenvironmental Engineering* **133**(4), 381–392

Bray, J.D., Macedo, J. and Travasarou, T. (2018). Simplified procedure for estimating seismic slope displacements for subduction zone earthquakes. *Journal of Geotechnical and Geoenvironmental Engineering* **144**(3), 04017124

Cho, Y. and Rathje, E.M. (2022). Generic predictive model of earthquake-induced slope displacements derived from finite-element analysis. *Journal of Geotechnical and Geoenvironmental Engineering* **148**(4), 04022010

Duncan, J.M., Wright, S.G. and Brandon, T.L. (2014). *Soil strength and slope stability*. John Wiley & Sons, Hoboken NJ, USA

Idini, B., Rojas, F., Ruiz, S. and Pastén, C. (2017). Ground motion prediction equations for the Chilean subduction zone. *Bulletin of Earthquake Engineering* **15**(5), 1853-1880

Instituto Nacional de Normalización (2012). Diseño sísmico de edificios NCh433. Of 1996. Modificada en 2012.

Kramer, S.L. (1996). *Geotechnical earthquake engineering*. Prentice-Hall International Series in Civil Engineering and Engineering Mechanics. Upper Saddle River, New Jersey, USA.

Ministerio de Minería (2018). Estudios de normativas internacionales de diseño, construcción, operación, cierre y post cierre de depósitos de relaves. Santiago, Chile

Ministerio de Minería (2007). Decreto Supremo 248. Reglamento para la aprobación de proyectos de diseño, construcción, operación y cierre de los depósitos de relaves. 29 de diciembre de 2006. Santiago, Chile

Ministerio de Minería (1970). Decreto 86. Reglamento de construcción y operación de tranques de relaves. 31 de julio de 1970. Santiago, Chile

Ministerio de Obras Públicas (2020). Manual de Carreteras. Volumen 3: Instrucciones y criterios de diseño. Santiago, Chile

Ministerio de Obras Públicas (2015). Decreto 50. Aprueba reglamento a que se refiere el artículo 295 inciso 2º, del Código de Aguas, estableciendo las condiciones técnicas que deberán cumplirse en el proyecto, construcción y operación de las obras hidráulicas identificadas en el artículo 294 del referido texto legal. 13 de enero de 2015. Santiago, Chile

Ministerio de Vivienda y Urbanismo (2011). Decreto 61. Aprueba reglamento que fija el diseño sísmico de edificios y deroga decreto Nº117, de 2010. Diario Oficial de la República de Chile. Santiago, Chile

Noda, S. and Uwabe, T. (1976). Relation between seismic coefficient and ground acceleration for gravity quay walls. *6th World Conference on Earthquake Engineering*. New Delhi, India, vol. 2, 1963-1968

Ruiz, S. and Madariaga, R. (2018). Historical and recent large megathrust earthquakes in Chile. *Tectonophysics* **733**, 37-56

Saragoni, G.R. (1993). Análisis del riesgo sísmico para la reconstrucción del Puerto de Valparaíso. *6tas Jornadas Chilenas de Sismología e Ingeniería Antisísmica*, Universidad de Chile y ACHISINA, Santiago, Chile, vol. 2, 165-178

Saragoni, G.R. y Garrido, B. (2022). Coeficientes sísmicos estáticos para estudios de estabilidad de tranques de relaves para terremotos subductivos intraplaca chilenos. *Obras y Proyectos* **31**, 16-19

Seed, H.B. (1979). Considerations in the earthquake-resistant design of earth and rockfill dams. *Géotechnique* **29**(3), 215-263

Seed, H.B. and Martin, G.R. (1966). The seismic coefficient in earth dam design. *Journal of the Soil Mechanics and Foundations Division* **92**(3), 25-58

Sernageomin (2024). Catastro de depósitos de relaves en Chile 2023. Gobierno de Chile, Servicio Nacional de Geología y Minería. Retrieved from: https://www.sernageomin.cl/datos-publicos-deposito-de-relaves/. August 2024.

Sernageomin (2016). Guía para el cumplimiento de DS248 Depósitos de relaves bajo producción de 5000 tpm. Servicio Nacional de Geología y Minería, Gobierno de Chile, Santiago, Chile

Tang, L., Liu, X., Wang, X., Liu, S. and Deng, H. (2020). Statistical analysis of tailings ponds in China. *Journal of Geochemical Exploration* **216**, 106579

US Army Corps of Engineers. (2019). National inventory of dams (NID). https://nid.sec.usace.army.mil

Williams, D.J. (2021). Lessons from tailings dam failures—Where to go from here? *Minerals* **11**(8), 853

Statements & declarations

Funding

Support for this research was provided by the ANID FONDECYT Grant Nº1240744 and the Advanced Mining Technology Center (AMTC PIA ANID grant AFB230001).

Competing interests

All authors declare they have no financial interests

Author contributions

The information presented and analyzed in this study was provided by the Department of Mine Safety of the National Geology and Mining Service (Sernageomin). All authors contributed and approved the final manuscript.

Data availability

All data used during the study appear in the submitted article.

Annex. Table A1: Tailings dams database

#	kh_{OBE}	kh_{MCE}	kv_{OBE}	kv_{MCE}	Method	Year	Height	Volume	PGA_{OBE}	PGA_{MCE}	Class	Seismic Zone	OBE Mechanism	MCE Mechanism	FoS_{OBE}	FoS_{MCE}	FoS_{ST}	Status	Type	Const. Method
	(-)	(-)	(-)	(-)			(m)	(10^6 m^3)	(g)	(g)					(-)	(-)	(-)			
1	0,22	0,3			1	2018	23	0,05	0,86	1,11	B	3	Interface	Interface	1,3	1,14		Ac	Em	DS
2		0,16			5	2016	9	0,05		0,16	A	3				1,2	2,16	Ac	Em	DS
3	0,22				Unspecified	2008	6	0,57			A	3			1,777		1,928	In	SD	DS
4	0,15	0,2			6	2015	10	0,05	0,4		A	3			1,39	1,23	3,5	Ac	Em	DS
5	0,1				2	1986	10	0,04			A	3						In	SD	US
6		0,2			3	2015	8	0,004			A	3			1,27	1,27		Ac	SD	CL
7		0,224			1	2015	156,5	375,71		1,05	C	3	Inslab			1,2	1,9	Ac	Em	DS
8	0,14	0,2			1	2016	137	2192,00	0,4	0,68	C	3	Interface	Inslab	1,21	1,23	1,82	Ac	Em	DS
9	0,12	0,18			7	2016	15,7	0,41			B	3			1,336	1,215	1,648	In	SD	DS
10	0,12	0,2			7	2016	18	0,94			B	3			1,481	1,279	1,89	In	SD	DS
11	0,15				Unspecified	2016	18,5	0,05	0,5		B	3			1,3		1,8	Ac	Em	DS
12	0,12	0,2			7	2016	9,82	2,40			B	3			1,796	1,554	2,297	In	SD	CL
13	0,12	0,15			1	2021	31	1,63	0,249	0,373	C	3			1,4	1,2	1,8	In	SD	CL
14	0,07	0,11			1	2018	54	3,88	0,249	0,373	C	3			1,78	1,65	2,04	Ac	SD	CL
15	0,21				5	2018	9,5	0,27	0,32		A	3			1,43		2,22	In	Em	DS
16		0,2		0,13	Unspecified	2016	73	68,97		0,56	C	3				1,2	1,7	Ac	Em	CL
17		0,19			3	2017	28	0,44	0,38		B	3	Interface		1,347	1,347	2,37	Ac	SD	DS
18	0,12	0,16		0,1	1	2022	90	92,13			C	3						Ac	Fi	Te
19	0,2				1	2021	6	6,67	0,72		B	3	Interface					Ac	Em	DS
20	0,11	0,15			1	2021	14		0,38	0,51	A	3			1,25	1,2	1,56	Ac	Em	DS
21	0,12	0,15		0,1	1	2015	68	5,33	0,39	0,5	C	3			1,342	1,231	1,761	In	SD	DS
22		0,2			3	2018	6				A	3			1,212	1,212		In	Po	Ot
23	0,14		0,09		1	2016	49		0,472	0,996	C	3	Interface	Inslab	1,72		2,5	Ac	Fi	Te
24	0,04	0,15			Unspecified	2018	5				A	3						Ac	Em	DS
25		0,2			3	2019	6				A	3			1,2	1,2	1,363	Ac	Fi	Te
26		0,2			3	2016	5				A	3						Ac	Fi	Te
27	0,12				5	2022	6,5				A	3			1,61		2,1	In	Em	DS
28	0,072	0,14			1	2021	30	2,75	0,24	0,41	C	3	Inslab	Inslab		2,1	3,3	Ac	Em	CL
29	0,12	0,19			1	2018	80		0,4	0,63	C	3	Inslab	Inslab	1,8	1,5	2,7	Ac	SD	CL
30	0,1107	0,2			1	2018	12,5	0,57	0,369		A	3	Interface	Interface	1,485	1,227	1,856	In	Fi	DS
31	0,12	0,15			1	2015	66	15,54	0,39	0,5	C	3			1,4	1,29	1,85	Ac	Em	DS
32	0,144	0,196			1	2019	11		0,48	0,708	A	3			1,48	1,06	2,56	Ac	Em	DS

33	0,15	0,19			1	2017	67	14,20	0,471	0,691	C	3			1,684	1,52	2,821	Ac	SD	DS
34	0,07	0,15			1	2021	16				B	3			1,494	1,262	1,756	Ac	Fi	Te
35	0,16		0,09		1	2019	11	0,02	0,54		A	3			1,2		1,47	Ac	SD	CL
36	0,2	0,22			1	2021	10	0,06	0,8	1	A	3	Interface	Interface	1,249	1,205	1,885	Ac	Em	DS
37		0,2		0,1	3	2022	5	0,06			A	3			1,22	1,22		Ac	Em	DS
38	0,15				Unspecified	2002	39				C	3			1,21		1,74	In	SD	CL
39		0,32			4	2019	11		0,32		A	3			1,7	1,7	2,3	Ab	SD	DS
40		0,2			3	2020	6				A	3			1,22	1,22	1,67	Ac	Po	Ot
41	0,05	0,12			1	2020	5		0,18	0,4	A	3			1,515	1,258	1,821	Ac	Em	DS
42	0,13				2	2009	57,5	29,33	0,31	0,61	C	3	Interface	Interface				In	Em	DS
43	0,104				2	2021	8				A	3						Ac	Em	DS
44	0,15				11	2016	5				A	3			1,24		3,52	Ab	Em	DS
45		0,19			Unspecified	2016	31	7,11		0,401	C	3				1,3	2,2	Ac	Em	DS
46		0,2			3	2006	25,5	4,99	0,4		B	3	Interface		1,25	1,25	1,91	Ac	Pa	DS
47	0,17	0,21			1	2017	90	12,23	0,522	0,646	C	3			1,694	1,622	3,044	Ac	Fi	Te
48		0,15			1	2005	150	297,00		0,41	C	3		Interface		1,2	1,6	Ac	Em	DS
49	0,16	0,21			1	2008	80	11,73	0,53	0,81	C	3	Inslab	Interface		1,2	2,2	Ac	SD	DS
50		0,2			3	2017	30	1,88	0,33	0,44	C	3	Interface	Interface	1,4	1,4		Ac	SD	CL
51		0,32			4	2014	9	0,004			A	3			1,52	1,52		In	Em	US
52		0,32			4	2014	5	0,01	0,4		A	3			2,166	2,166		Ac	Em	DS
53		0,2			3	2016	10	0,03	0,4		A	3			1,363	1,363	1,93	Ac	Em	DS
54		0,32			4	2015	11	0,10	0,32		A	3			1,8	1,8	2,4	Ac	SD	DS
55	0,17	0,21			1	2013	52,9	53,53	0,522	0,646	C	3			1,514	1,404	2,417	Ac	SD	CL
56	0,18				1	2020	60	26,28	0,478	0,544	C	3			1,27	1,16	2,07	Ac	Fi	Te
57	0,084	0,16	0,056	0,11	1	2012	35,5	8,27	0,28	0,54	C	3	Interface	Interface		1,4	1,92	Ac	Em	DS
58		0,22			6	2016	15	0,21		0,6	B	3				1,2	2	In	SD	DS
59	0,1				2	1985	14	0,23			A	3						In	SD	US
60	0,1				2	1985	6	0,003			A	3						In	SD	US
61	0,1				2	1985	5	0,03			A	3						In	SD	US
62	0,2	0,28			1	2019	7,5	0,19	0,66	1,22	A	3	Interface	Interface	1,32		2,95	Ac	SD	Te
63		0,224			1	2014	157	337,08		1,05	C	3	Inslab	Inslab		1,2	1,7	Ac	Em	DS
64	0,1				2	1987	8	0,03			A	3						Ab	SD	CL
65		0,13			1	2017	5			0,42	A	3		Interface		1,605	2,82	Ac	Em	DS
66	0,1				2	1990	8	0,05			A	3						Ab	SD	CL
67	0,1389				2	1995	4,5	0,004			A	3						In	Em	DS
68		0,2			3	2017	10	0,02			A	3			1,25	1,25	1,46	In	SD	DS
69	0,15	0,22	0,1	0,15	1	2020	40	271,99	0,45	0,89	C	3	Inslab	Inslab	1,8	1,4	2,88	Ac	Em	DS
70		0,2		0,1	3	2016	30	1,27			C	3			1,56	1,56	2,34	Ac	Em	DS
71		0,2			3	2013	5				A	3						In	Po	Ot

72	0,12	0,2			6	2021	15	0,03	0,4		B	3			1,434	1,3		In	SD	DS
73	0,2	0,22			1	2012	13	0,03	0,8	1	A	3	Interface	Interface	1,303	1,264	1,836	Ac	SD	CL
74		0,16		0,11	1	2017	15	0,03		0,54	B	3		Interface		1,1	1,52	In	SD	DS
75	0,1				2	1989	20	0,01			B	3						In	SD	DS
76	0,08	0,15			1	2016	55,5	196,00	0,27	0,51	C	3	Inslab	Inslab	1,4	1,2	1,7	In	Em	DS
77	0,1				2	2002	12	0,27			A	3						In	SD	CL
78	0,11				5	2004	63,4	1,67	0,17		C	3			1,23			In	SD	CL
79	0,15	0,21			1	2020	43	0,62	0,46	0,67	C	3	Inslab	Inslab	1,67	1,43	2,87	Ac	Fi	Te
80	0,18				6	2017	15	0,24			B	3			1,885	1,26		Ac	Em	DS
81		0,16			9	2018	167	156,67		0,957	C	3		Inslab		1,2	2,5	Ac	SD	Ot
82		0,2		0,12	3	2019	8	0,07	0,33	0,6	A	3			1,224	1,224	2	In	SD	CL
83	0,072	0,14	0,047	0,09	1	2021	12	0,53	0,24	0,41	A	3	Inslab	Inslab		1,2	1,7	Ac	SD	CL
84		0,4			4	2017	6,5				A	3			1,782	1,782	3,123	In	Po	Ot
85	0,17	0,22	0,1	0,15	1	2010	8	3,03	0,564	0,984	B	3	Inslab	Inslab	1,84	1,8	3,95	Ac	SD	DS
86		0,32			4	2016	5				A	3			1,25	1,25	1,69	Ab	Em	DS
87		0,32			4	2016	15	0,03			B	3			1,8	1,8	2,4	Ac	SD	CL
88	0,14	0,19			1	2019	34,76	18,42	0,47	0,69	C	3			1,7	1,5	2,67	Ac	SD	CL
89		0,22		0,15	1	2016	24,5	4,07			B	3				1,4	2,2	In	SD	CL
90	0,1				2	1983	14	0,15			A	3						In	SD	CL
91		0,22		0,15	1	2016	12	5,87			B	3				1,4	2,2	In	SD	DS
92	0,05	0,12			Unspecified	2020	29	380,00	0,42	0,48	C	2	Inslab	Inslab		1,65	2,75	Ac	Em	CL
93	0,1				2	1988	8	0,04			A	3						In	SD	US
94		0,22		0,15	1	2014	25,5	10,22		0,996	B	3		Inslab		1,4	2,3	Ac	Em	CL
95	0,2	0,37			5	2018	52	6,38	0,49	0,929	C	3			1,58	1,07	3,15	Ac	SD	DS
96	0,1				2	1987	5	0,03			A	3						In	SD	CL
97	0,1				2	1987	6	0,02			A	3						Ab	SD	CL
98		0,2			3	2016	9,3	0,01	0,4		A	3			1,28	1,28	1,92	Ac	Em	DS
99	0,15	0,24			5	2011	14,65	0,36	0,22	0,48	A	3			1,28	1,24	1,9	Ac	Em	DS
100	0,1				6	2016	51	242,67	0,3		C	2			1,5		2,8	Ac	SD	Ot
101	0,16	0,25			1	2018	14,6	0,24	0,548	1,47	A	2	Inslab	Inslab	1,5	1,27	2,1	In	Em	DS
102	0,13	0,2	0,08	0,13	1	2020	12	1,40	0,42	0,72	A	2	Inslab	Inslab	1,4	1,2	2,1	Ac	Fi	DS
103	0,08	0,2			8	2022	8,79	0,18		0,658	A	2				1,41	2,79	In	Em	DS
104	0,12				1	2010	30	0,76			C	2			1,29		1,65	In	Em	DS
105	0,1				2	1987	12	3,16			B	3						In	SD	CL
106		0,18			1	2015	42	14,96	0,34	0,62	C	2	Inslab	Inslab		1,24	1,82	Ac	Em	DS
107		0,15		0,1	10	2018	156	468,75		0,88	C	2		Interface		1,26	1,79	Ac	Em	DS
108	0,14	0,21	0,09	0,14	1	2021	50	3000,00	0,45	0,86	C	2	Inslab	Inslab	1,47	1,2	2,26	Ac	Em	DS
109	0,13	0,15			1	2010	288	318,40	0,42	0,48	C	2			1,28	1,23	1,72	Ac	Em	DS
110	0,104				2	2017	4	0,02			A	3					1,56	In	SD	DS

111	0,15	0,17			9	2016	190	689,66		1,2	C	2	Inslab	Inslab	1,37	1,31	2,16	Ac	SD	DS
112		0,3		0,2	Unspecified	2009	60	22,00		0,51	C	2		Shallow crustal		1,39		Ac	SD	DS
113	0,105	0,17			1	2020	310	0,000	0,35	0,56	C	2	Inslab	Inslab		2,43	3,96	Ac	SD	CL
114		0,13		0,09	1	2021	26,47			0,43	B	2		Inslab		1,38	1,88	Ac	Em	DS
115	0,05	0,15			Unspecified	2002	27	9,87			B	2						In	Fi	Te
116	0,1				2	1997	18	0,12			B	3			1,23		2,33	Ab	SD	CL
117		0,32			4	2014	8	0,01			A	3						Ab	SD	CL
118	0,14				1	2019	54	504,70	0,45		C	2			1,2		1,8	Ac	SD	DS
119		0,165		0,11	1	2021	52	1451,00		0,55	C	2		Inslab		1,4	2	Ac	Em	Ot
120	0,16	0,25			1	2016	45	1,35	0,548	1,47	C	2	Inslab	Inslab	1,13	1,03	1,5	In	Em	DS
121	0,11	0,2			1	2012	10	0,67	0,38	0,79	A	2	Inslab	Interface	1,323	1,144	1,747	In	Em	DS
122	0,13	0,16	0,04	0,05	1	2014	13	2,18	0,445	0,537	B	1			1,5	1,36	2,3	In	Fi	Te
123	0,12	0,15	0,04	0,05	8	2021	77	763,53	0,271	0,903	C	1	Inslab	Inslab				Ac	Em	DS
124	0,072	0,114			1	2018	37,2	14,80	0,24	0,38	C	1	Inslab	Inslab	1,4	1,2	1,7	Ac	Fi	Te
125	0,15	0,2			5	2010	23	6,65	0,09	0,54	B	1	Shallow crustal	Interface	1,359	1,218	1,986	In	Em	DS

Method: Method number according to Table 4. Status: Active (Ac), Inactive (In), Abandoned (Ab). Type: Embankment (Em), Sand Dam (SD), Filtered (Fi), Paste (Pa), Pool (Po). Constructive Method: Downstream (DS), Centerline (CL), Terrace (Te), Upstream (US), Other (Ot)